Intense Photosensitized Emission from Stoichiometric Compounds Featuring Mn^{2+} in Seven- and Eightfold Coordination Environments

Howard O. N. Reid and Ishenkumba A. Kahwa*

Chemistry Department, University of the West Indies, Mona Campus, Kingston 7, Jamaica

Andrew J. P. White and David J. Williams

Chemical Crystallography Laboratory, Chemistry Department, Imperial College of Science, Technology and Medicine, South Kensington, London SW7 2AY, U.K.

Received January 13, 1998

Synthetic, structural and luminescence studies of stoichiometric crown ether compounds of Mn^{2+} in well-defined coordination environments were undertaken in an effort to understand the origin of emitting crystal defects found in cubic *F23* $[(K18C6)_4MnBr_4][TlBr_4]_2$ crystals (Fender, N. S.; et al. *Inorg. Chem.* **1997**, *36*, 5539). The new compound $[Mn(12C4)_2][MnBr_4]_2[N(CH_3)_4]_2$ (**3**) features Mn^{2+} ions in eight- and fourfold coordination environments of $[Mn(12C4)_2]^{2+}$ and $MnBr_4^{2-}$ respectively, while Mn^{2+} in $[Mn(15C5)(H_2O)_2][TlBr_5]$ (**4**) is in the sevenfold coordination polyhedron of $[Mn(15C5)(H_2O)_2]^{2+}$. Crystal data for **3**: monoclinic, $P2_1/c$ (No. 14); $a = 14.131(3)$ Å, $b = 12.158(1)$ Å, $c = 14.239(2)$ Å, $\beta = 110.37(1)°$, $Z = 2$, R1 = 0.039 and wR2 = 0.083. For **3**, long-lived emission (77 K decay rate $\simeq 3 \times 10\ s^{-1}$) from $[Mn(12C4)_2]^{2+}$ (the first for eight-coordinate Mn^{2+} in stoichiometric compounds) is observed ($\lambda_{max} \simeq 546$ nm) along with that of the sensitizing $MnBr_4^{2-}$ ($\lambda_{max} \simeq 513$ nm), which is partially quenched. Emission from the seven-coordinate $[Mn(15C5)(H_2O)_2]^{2+}$ species of **4** and $[Mn(15C5)(H_2O)_2][MnBr_4]$ (the first for seven-coordinate Mn^{2+} in stoichiometric compounds) peaks at $\lambda_{max} \simeq 592$ nm. Unusually intense absorptions attributable to the seven-coordinate species are observed at 317 ($^2T_2(^2I) \leftarrow {}^6A_1$), 342 ($^4T_1(^4P) \leftarrow {}^6A_1$), 406 ($^4E(^4G) \leftarrow {}^6A_1$), and 531 ($^4T_1(^4G) \leftarrow {}^6A_1$) nm.

Introduction

Strong luminescence from the $^4T_1(^4G)$ state of Mn^{2+} ions in O_h (red) and T_d (green) oxide coordination environments is the basis of successful applications of manganese(II) in commercial phosphors.[1−4] However, violet (≃425 nm),[5] blue (≃460 nm),[6,7] and orange (≃590 nm)[8−10] emissions from Mn^{2+} ions doped in crystalline or amorphous materials have also attracted much attention. Whereas intensive spectroscopic studies of many Mn^{2+}, doped oxides,[9,11−15] oxo salts,[5,9,14] sulfides,[8,9,14] and halides[9,15−19] have revealed interesting information on the Mn^{2+} electronic response to changing ligand field, detailed interpretation of these data is difficult because of uncertainties in the nature (location and symmetry) of the emitting Mn^{2+} site. Besides these ambiguities, doping often leads to crystal defects which further complicate luminescence behavior through electronic interactions with the Mn^{2+} ions or by their own emission.[16,17] Therefore, in order to understand the emission characteristics of Mn^{2+} in non-O_h and -T_d environments, it is desirable to study stoichiometric manganese(II) compounds with well-defined Mn^{2+} coordination sites which exhibit the luminescence characteristics of interest. However, to our knowledge, emission from stoichiometric manganese compounds featuring Mn^{2+} in coordination environments other than O_h and T_d, or their distorted derivatives, is very rare.

Our interest in this problem was inspired by the unusual crystal defect yellow emission centered at about 570 nm, which is efficiently sensitized by $MnBr_4^{2-}$, in the supramolecular system $[(A18C6)_4MnBr_4][TlBr_4]_2$ (**1** (A = K, NH_4^+; 18C6 = 18-crown-6)); the rubidium analogue, $[(Rb18C6)_4MnBr_4][TlBr_4]_2$ (**2**), exhibits normal T_d $MnBr_4^{2-}$ spectra and much weaker defect luminescence behavior.[20,21] In an attempt to

* Author to whom correspondence should be addressed (Fax, 876-977-1835; e-mail, ikahwa@uwimona.edu.jm).

(1) Morell, A.; Khaiti, N. E. *J. Electrochem. Soc.* **1993**, *140*, 2019.
(2) Barthou, C.; Benoit, J.; Benalloul, J. *J. Electrochem. Soc.* **1994**, *141*, 524.
(3) Collins, B. T.; Ling, M. *J. Electrochem. Soc.* **1993**, *140*, 1752.
(4) DeMarsh, L. *SMPTE J.* **1993**, 1095.
(5) Kaplanová, M.; Trojan, M.; Brandová, D.; Navrátil, J. *J. Lumin.* **1984**, *29*, 199.
(6) Yamada, H.; Matsukiyo, H.; Suzuki, T.; Yamada, H.; Yamamoto, H.; Okamura, T.; Imai, T.; Morita, M. *Proc.—Electrochem. Soc.* **1988**, *88-24* (*Proc. Symp. Lumin. Sci. Technol.* **1988**, 184−9).
(7) Tokyo Shibaura Electric Co., Ltd. Fr. 2,047,526 (Cl. C 09K), March 12, 1971, Japan Appl. May 8, 1969; 17 pp.
(8) Collins, B. T.; Ling, M. *J. Electrochem.* **1993**, *140*, 1752.
(9) Palumbo, D. T.; Brown, J. J. *J. Electrochem.* **1971**, *118*, 1159.
(10) Singh, G.; Singh, L. K. *Ind. J. Pure Appl. Phys.* **1984**, *22*, 743.
(11) Bartthou, C.; Benoit, J.; Benalloul, P.; Morell, A. *J. Electrochem. Soc.* **1994**, *141*, 524.
(12) Morell, A.; Khiati, N. E. *J. Electrochem. Soc.* **1993**, *140*, 2019.
(13) Shea, L. E.; Dalta, R. K.; Brown, J. J. *J. Electrochem. Soc.* **1994**, *141*, 1950.
(14) Peters, T. E.; Pappalardo, R. G.; Hunt, R. B. *J. Lumin.* **1984**, *31/32*, 290.
(15) Palumbo, D. T.; Brown, J. J. *J. Electrochem.* **1970**, *117*, 1185.
(16) McKeever, S. W. S.; Jassemnejad, B.; Landreth, J. F. *J. Appl. Phys.* **1986**, *60*, 1125.
(17) Lewandowski, A. C.; Wilson, T. *M. Phys. Rev. B* **1984**, *50*, 2780.
(18) Goode, D. H. *J. Chem. Phys.* **1965**, *43*, 2830.
(19) Pappalardo, R. *J. Chem. Phys.* **1959**, *31*, 1050.
(20) Fender, N. S.; Fronczek, F. R.; John, V.; Kahwa, I. A.; McPherson, G. L. *Inorg. Chem.* **1997**, *36*, 5539.
(21) Fender, N. S.; Finegan, S. A.; Miller, D.; Mitchell, M.; Kahwa, I. A.; Fronczek, F. R. *Inorg. Chem.* **1994**, *33*, 4002.

S0020-1669(98)00035-4 CCC: $15.00
Published on Web 07/27/1998

understand the nature of the defect emitter in **1,** we sought to prepare relatively simple manganese compounds with well-defined noncubic Mn^{2+} coordination environments and study their luminescence spectroscopic characteristics and decay dynamics. It was hoped that these studies would shed new light on the origin of the intriguing emission behavior of supramolecular system **1** while opening new opportunities for probing Mn^{2+} sites in complex coordination environments, such as those of industrial minerals[22−24] and compounds.[25] Crown ether and $MnBr_4^{2-}$ compounds were targeted because of our interest in system **1** as well as the simplicity and flexibility of the crown ether framework, which adapts to a variety of coordination requirements.[26]

Herein we report the preparation, crystal structures, and luminescence behavior of new compounds $[Mn(12C4)_2][MnBr_4]_2[N(CH_3)_4]_2$ (12C4 = 12-crown-4) (**3**) and $[Mn(15C5)(H_2O)_2][TlBr_5]$ (15C5 = 15-crown-5) (**4**), which feature Mn^{2+} in eight- and sevenfold coordination environments.

Experimental Section

Materials. The materials used, their purity, and sources are as follows: magnesium, manganese, and zinc bromides, Analar, BDH; tetramethylammonium bromide, 99%, Matheson Coleman and Bell; 12-crown-4, 98%, and 15-crown-5, 98%, Aldrich; thallium bromide was obtained by neutralizing pure thallium(III) oxide (99.99%, Aldrich) with hydrobromic acid (99.999%, Aldrich). The solvents used were reagent grade.

Elemental Analysis. Bromine, carbon, hydrogen, and nitrogen analyses were performed by MEDAC Ltd., Brunel Science Center, Egham, Surrey, U.K. Magnesium, manganese, and zinc analyses were obtained using an atomic absorption spectrometer described previously.[26]

Luminescence Decay Dynamics and Spectroscopic Studies. The Perkin-Elmer LS5 fluorescence spectrometer, the Photon Technology PL 2300 nitrogen and PL 201 dye lasers, and the homemade computational programs used were described previously.[26] Variable-temperature measurements (10−320 K) were carried out using our new APD Cryogenics Inc. CSW-202 Displex helium refrigerator system with the sample in contact with cryocon conducting grease.

Syntheses. $[Mn(15C5)(H_2O)_2][TlBr_5]$ (4). $MnBr_2 \cdot 4H_2O$ (1 mmol), thallium tribromide (1 mmol), and 15C5 (1 mmol) were mixed in 120 cm^3 of a 3:1 dichloromethane/methanol mixture and then refluxed overnight, yielding a clear solution; thallium(III) bromide dissolves slowly. Hydrobromic acid (5 cm^3) was added, and the solution was decanted into a 250 cm^3 conical flask and allowed to evaporate slowly on a warm hot plate until lime-green crystals were deposited. The crystals were harvested and dried by being rolled quickly and gently on tissue paper; yield ≃61%. Anal. Calcd for **4** $\cdot 1.5H_2O$ ($Br_5C_{10}H_{27}MnO_{8.5}Tl$): C, 12.7; H, 2.9. Found: C, 12.48; H, 2.56.

$[Mn(15C5)(H_2O)_2][MnBr_4] \cdot 2H_2O$ (5). $MnBr_2 \cdot nH_2O$ (2 mmol) and 15C5 (1 mmol) were mixed in 40 cm^3 of methanol, from which **5** was crystallized by vapor diffusion using diethyl ether in a desiccator that contained silica desiccants. Anal. Calcd for $Br_4C_{10}H_{28}Mn_2O_9$: Br, 44.3; C, 16.64; H, 3.91. Found: Br, 43.84; C,16.67; H, 3.64.

$[Mn(15C5)(H_2O)_{2-x}(D_2O)_x][TlBr_5] \cdot ((H_2O)_{2-x}(D_2O)_x)$ ($0 < x < 2$) (6). Deuterate **6** was prepared by suspending compound **4** in D_2O and evaporating to dryness the resulting mixture in a desiccator containing concentrated sulfuric acid. The dry compound was subsequently kept in a sealed glass tube.

$[Mn(12C4)_2][MnBr_4]_2[N(CH_3)_4]_2$ (3), $[Mn(12C4)_2][MnBr_4]_x[ZnBr_4]_{2-x}[N(CH_3)_4]_2$ (7), and $[Mg(12C4)_2]_{1-x}[Mn(12C4)_2]_x[MnBr_4]_2[N(CH_3)_4]_2$ (8). $MnBr_2 \cdot nH_2O$ (3 mmol), 12C4 (2.06 mmol), and tetramethylammonium bromide (2 mmol) were dissolved in a 3:1 acetonitrile/methanol mixture and refluxed overnight. The solution was then decanted into a 250 cm^3 conical flask and slowly evaporated on a hot plate. After 24 h large crystals were deposited. The crystals were harvested and dried by being rolled quickly and gently in tissue paper. Compounds **7** and **8** were prepared in a similar manner using 1 mmol of $MnBr_2 \cdot nH_2O$ and 2 mmol of $ZnBr_2 \cdot nH_2O$ or 2 mmol of $MnBr_2 \cdot nH_2O$ and 1 mmol of $MgBr_2 \cdot nH_2O$, respectively. The preparation procedure for **8** was repeated with 2.5 mmol of $ZnBr_2 \cdot nH_2O$ to obtain crystals of **9** (vide infra). Crystal colors and yields are as follows: **3**, lime-green, 72%; **7**, light-green, 64%; **8**, yellow-green, 70%. Anal. for **3**. Calcd for $Br_8C_{24}H_{56}Mn_3N_2O_8$: Br, 49.0; C, 22.1; H, 4.3; N, 2.1. Found: Br, 48.7 (average of several analyses in the range 48.3−49.9); C, 21.87; H, 4.32; N, 2.17. Anal. for **7**. Calcd for $Br_8C_{24}H_{56}MnN_2O_8Zn_2$: C, 21.8; H, 4.3; Mn, 4.1; N, 2.1; Zn, 9.9. Found: C, 22.3; H, 4.39; Mn, 4.31; N, 2.28; Zn, 10.4. Anal. for **8**. Calcd for $Br_8C_{24}H_{56}MgMn_2N_2O_8$: C, 22.6; H, 4.4; Mg, 1.9; Mn, 8.6; N, 2.2. Found: C, 22.33; H, 4.40; Mg, 1.80; Mn, 8.9; N, 2.18. Anal. for **9**. Calcd for $Br_8C_{24}H_{56}MnN_2O_8Zn_2$: C, 21.8; H, 4.3; Mn, 4.1; N, 2.1; Zn, 9.9. Found: C, 21.75; H, 4.26; Mn, 3.80; N, 2.28; Zn, 10.4.

Structural Determination. Data for **3** were collected on a Siemens P4/PC diffractometer using graphite-monochromated Mo Kα (λ = 0.71073 Å) radiation and ω scans. The structure was solved by direct methods and refined by full-matrix least squares based on F^2. The H atoms were placed in calculated positions, assigned isotropic thermal parameters, $U(H) = 1.2U_{eq}(C)$ [$U(H) = 1.5U_{eq}$(C-Me)], and allowed to ride on their parent atoms. Computations were carried out using the SHELXTL PC program system (version 5.03, Siemens Analytical X-Ray Instruments, Inc., Madison, WI, 1994). Essential data for **3**: empirical formula = $Br_8C_{24}H_{56}Mn_3N_2O_8$; formula weight = 1304.81; T = 293(2) K; crystal system = monoclinic; space group = $P2_1/c$ (No. 14); unit cell dimensions, a = 14.131(3) Å, b = 12.158(1) Å, c = 14.239(2) Å, β= 110.37(1)°; Z = 2; number of reflections = 3739; data = 3596; final R indices [$I > 2\delta(I)$], R1 = 0.039, wR2 = 0.083. All other structural data are given as Supporting Information.

Results and Discussion

Syntheses and Structure. Direct preparation of compounds **3**, **7**, and **8** as good-quality crystals is straightforward and of high yield. The single-crystal X-ray diffraction study of **3** (Figure 1) confirms the formation of the sandwich compound, $[Mn(12C4)_2][MnBr_4]_2[N(CH_3)_4]_2$. One of the manganese atoms, which coordinates to the 12C4 macrocycle, is positioned on a crystallographic inversion center. The macrocycle has approximate molecular C_4 symmetry, i.e., all four oxygen atoms lying on one face of the crown are coplanar to within 0.08 Å and are bound to the manganese atom which adopts a perching geometry. The 12C4 molecule exhibits rotational disorder about its C_4 axis; two discrete 50% occupancy orientations rotated by about 36° were identified (Figure 2). The crown-complexed Mn atom is eight-coordinate, but because of the inversion center and the rotation disorder, it is not possible to distinguish between the two probable coordination geometries, i.e., square biprismatic and square antiprismatic. Indeed both geometries could coexist within the crystal, although only in approximately equal populations. The square biprismatic geometry is known for the similar iron(II) sandwich, $[Fe(12C4)_2]^{2+}$,[27] but the square antiprismatic geometry known for $[Mn(12C4)_2]^{2+}$ in $[Mn(12C4)_2][Br_3]_2$,[28] $[Na(12C4)_2]^+$,[29−31] and $[Ca(12C4)_2]^{2+}$ [32] is the

(22) Bakhterev, V. V.; Solomonov, I. V. *Inorg. Mater.* (Transl. of *Neorg. Mater.*) **1995**, *31*, 526.
(23) Kononov, O. V.; Nesterov, I. V. *Mineral. Geokhim. Vol' framovykh Mestorozhd., Tr. Vses. Soveshch., 3rd* **1975**, 364.
(24) Loh, E. *Am. Mineral.* **1975**, 60, 79.
(25) Knops-Gerrits, P.-P. H. J. M.; Schryver, F. C. D.; Auweraer, M. van der; Mingroot, H. V.; Li, X.; Jacobs, P. A. *Chem. Eur. J.* **1996**, *2*, 592.
(26) Fairman, R. A.; Gallimore, W. A.; Spence, K. V. N.; Kahwa, I. A. *Inorg. Chem.* **1994**, *33*, 823.
(27) Meir K.; Rihs, G. *Angew. Chem., Int. Ed. Engl.* **1985**, *24*, 858.
(28) Hughes, B. B.; Haltiwanger, R. C.; Pierpont, C. G.; Hampton M.; Blackmer, L. *Inorg. Chem.* **1980**, *19*, 1801.
(29) Remoortere, F. P. van; Boer, F. P. *Inorg. Chem.* **1974**, *13*, 2071.
(30) Boer, F. P.; Newman, M. A.; Remoortere, F. P. van; Steiner, E. C. *Inorg. Chem.* **1974**, *13*, 2826.

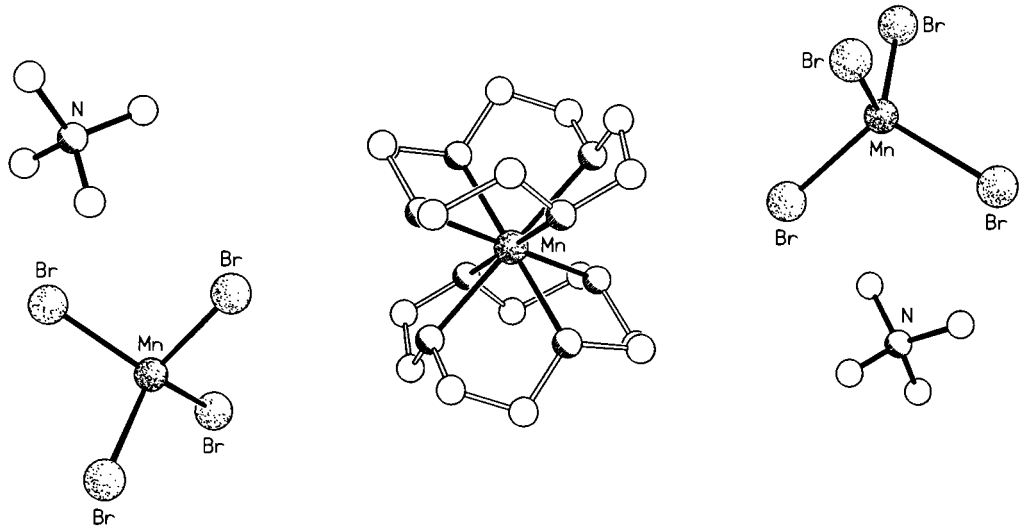

Figure 1. The crystal structure of $[Mn(12C4)_2][MnBr_4]_2[N(CH_3)_4]_2$ (**3**).

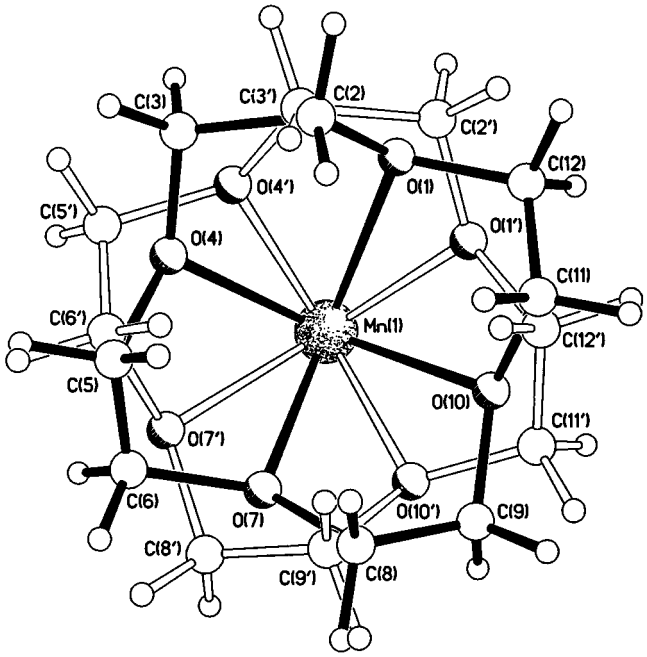

Figure 2. The two orientations of the 12C4 unit in **3**.

more frequently encountered conformation. The Mn−O distances are in the range 2.26(1)−2.42(1) Å for one of the 12C4 orientations and 2.24(1)−2.41(1) Å for the other. The Mn atom lies 1.34 and 1.31 Å out of the planes of each set of four oxygen atoms, respectively.

The $MnBr_4^{2-}$ anion lies in a general position within the unit cell and has roughly T_d symmetry typical for this species;[20,21] Mn−Br distances are in the range 2.494 (1)−2.515(1) Å and Br−Mn−Br angles in the range 107.4(1)−112.2(1)°. The tetramethylammonium cations are ordered with noncrystallographic T_d symmetry. The shorter through-space Mn−Mn separations between the two crystallographically independent manganese centers are 7.09 and 7.30 Å. The shortest separation of $MnBr_4^{2-}$ centers is 8.31 Å while that between the most proximal $[Mn(12C4)_2]^{2+}$ centers is 9.36 Å.

The crystal structure of $[Mn(15C5)(H_2O)_2][TlBr_5]$ (**4**) was determined. The nearly D_{3h} trigonal bipyramidal geometry of $TlBr_5^{2-}$ anions and the trans configuration of the two water molecules in the $[Mn(15C5)(H_2O)_2]^{2+}$ cation were evident, but extensive disorder of the 15C5 chelate made complete solution of the structure difficult.

Compounds **3** and **4** featuring well-defined noncubic Mn^{2+} coordination environments are, as desired, luminescent and indeed attractive for emission studies seeking to establish manganese(II) luminescence behavior beyond cubic crystal fields.

Luminescence Spectra of Compounds 3, 7, and 8. There are two potential sources of emission in $[Mn(12C4)_2][MnBr_4]_2[N(CH_3)_4]_2$ (**3**), namely, the Mn^{2+} species, $[Mn(12C4)_2]^{2+}$ and $MnBr_4^{2-}$. It was therefore prudent to attempt physical isolation of $[Mn(12C4)_2]^{2+}$ and $MnBr_4^{2-}$ species from each other and then study the luminescence behavior of each one of them in the absence of the other. It is well established[26,33] that the stability order for MX_4^{2-} anions (M = divalent element; X = halogen) is $ZnX_4^{2-} > MnX_4^{2-} > MgX_4^{2-}$. Therefore, in a preparative procedure similar to that of **3**, the presence of excess $ZnBr_2$ should transform manganese(II) to predominantly the sandwich $[Mn(12C4)_2]^{2+}$ while the formation of $MnBr_4^{2-}$ is suppressed in favor of $ZnBr_4^{2-}$. On the other hand, an excess of Mg^{2+} ions over Mn^{2+} should favor conversion of manganese(II) to mainly $MnBr_4^{2-}$ and magnesium(II) to the sandwich cation $[Mg(12C4)_2]^{2+}$. These expectations are indeed realized synthetically (see Experimental Section); reaction mixtures containing manganese(II) and zinc(II) bromides yield $[Mn(12C4)_2][MnBr_4]_x[ZnBr_4]_{2-x}[N(CH_3)_4]_2$ (**7**), while those containing manganese(II) and magnesium(II) bromides yield $[Mg(12C4)_2]_{1-x}[Mn(12C4)_2]_x[MnBr_4]_2[N(CH_3)_4]_2$ (**8**). Both elemental analysis (vide supra) and luminescence spectroscopy (Figure 3; T_d and T_g denote delay and gating times respectively) show (vide infra) that the magnitude of x in the stoichiometries of **7** and **8** is small but not 0.

Normally, $MnBr_4^{2-}$ ions exhibit green emission ($\lambda \simeq 510-535$ nm). Accordingly, the 77 K emission spectrum of **8**, for which the concentration of $MnBr_4^{2-}$ is much higher than that of $[Mn(12C4)_2]^{2+}$, exhibits largely normal $MnBr_4^{2-}$ emission peaking at ca. 530 nm with a weak shoulder toward the 550 nm region (Figure 3c). The excitation spectrum of **8** monitored at 514 nm features normal absorptions of $MnBr_4^{2-}$. However, the 77 K excitation spectrum of the long-wavelength emission of **8** monitored in the shoulder at 585 nm shows absorptions

(31) Remoortere, F. P. van; Boer, F. P.; Steiner, E. C. *Acta Crystallogr., Sect. B* **1975**, *31*, 1420.
(32) Rogers, R. D.; Voss, E. *Inorg. Chim. Acta* **1987**, *133*, 181.
(33) Blake, A. B.; Cotton, F. A. *Inorg. Chem.* **1964**, *3*, 5 and references therein.

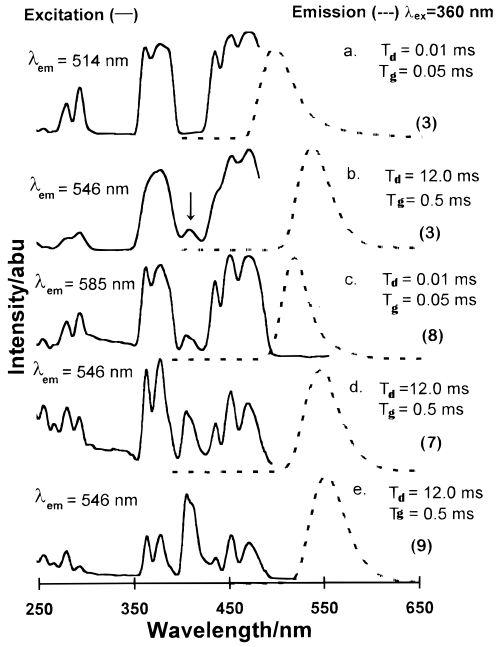

Figure 3. Time dependent uncorrected 77 K excitation and emission spectra of (a, b) $[Mn(12C4)_2][MnBr_4]_2[N(CH_3)_4]_2$ (**3**), (c) $[Mg(12C4)_2]_{1-x}[Mn(12C4)_2]_x[MnBr_4]_2[N(CH_3)_4]_2$ (**8**), (d) $[Mn(12C4)_2][MnBr_4]_x[ZnBr_4]_{2-x}$ $[N(CH_3)_4]_2$ (**7**), and (e) $[Mn(12C4)_2][MnBr_4]_x[ZnBr_4]_{2-x}$ $[N(CH_3)_4]_2$ from reaction mixture with excess Zn^{2+} (**9**). The arrow indicates the unusually intense absorption attributed to eight-fold-coordinated Mn^{2+} in $[Mn(12C4)_2]^{2+}$ in compounds **3**, **7**, **8,** and **9**.

typical of $MnBr_4^{2-}$ and an additional weak feature at 410 nm (see arrow in Figure 3) for which the ratio of areas at 400−420 nm (A_{410}) and 425−500 nm (A_{450}), A_{410}:$A_{450} \approx$ 1:14, is small.

To establish whether the unusual absorption at 410 nm and the long-wavelength emission shoulder are due to the sandwich $[Mn(12C4)_2]^{2+}$, we studied the emission characteristics of **7** in which the concentration of $[Mn(12C4)_2]^{2+}$ species is much higher than that of $MnBr_4^{2-}$. Upon excitation at 77 K and 360 nm, **7** exhibits weak emission at about 546 nm (Figure 3d), the excitation spectrum of which is dominated by $MnBr_4^{2-}$ absorptions similar to those of the long-wavelength emission of **8** (Figure 3c). However, the peak at 410 nm in **7** is more prominent with an intensity ratio of A_{410}:$A_{450} \approx$ 1:3 (Figure 3d) compared to a value of about 1:14 for **8** (Figure 3c)! This means that direct excitation of the $[Mn(12C4)_2]^{2+}$ species is inefficient and, without sensitization by $MnBr_4^{2-}$, emission from the eight-coordinate manganese(II) cations would be extremely weak. To firm up this interpretation, the proportion of $MnBr_4^{2-}$ anions in samples of type **7** was further minimized; a sample **9** from a reaction mixture containing a larger (2.5:1) than stoichiometrically required (2:1) $ZnBr_4^{2-}$:$MnBr_4^{2-}$ ratio was obtained and its emission behavior studied. The emission of **9** is indeed weak and dominated by the 546 nm peak; the unusual 410 nm absorption is now the dominant feature (A_{410}:$A_{450} \approx$ 1:1) in the excitation spectrum (Figure 3e). The unusual weak long-wavelength emissions from **7,** on one hand, and **8** and **9**, on the other, are thus sensitized by the relatively abundant and trace amounts of $MnBr_4^{2-}$, respectively. Guided by the benefit of knowledge of the luminescence behavior of $[Mn(12C4)_2]^{2+}$ and $MnBr_4^{2-}$ when mutual interference is minimal, we sought to establish if the more complex emission characteristics of **3** are consistent with this interpretation.

Indeed, excitation of the manganese(II) compound **3** in the near UV (360 nm), leads to very intense green-yellow emission at both 77 and 300 K which is time-resolvable into a short-lived component at 514 nm (Figure 3a) and an unusual long-lived one peaking at about 546 nm (Figure 3b). The excitation spectra (Figure 3a,3b) of both emission features (77 K) are dominated by electronic transitions typical of $MnBr_4^{2-}$ ions[34−36] except, again, for the unusually intense absorption at ca. 410 nm (peak on arrow, Figure 3b; A_{410}:$A_{450} \approx$ 1:10) in the excitation spectrum of the (long-lived) 546 nm emission. We conclude that the intense long-lived emission peaking at 546 nm is indeed from the sandwich $[Mn(12C4)_2]^{2+}$ cations and is efficiently sensitized by $MnBr_4^{2-}$ anions. Taken together, the luminescence behavior of compounds **3** and **7**−**9** means that there are active $MnBr_4^{2-}\cdots[Mn(12C4)_2]^{2+}$ electronic interactions which are responsible for the sensitized emission from $[Mn(12C4)_2]^{2+}$. On the basis of the spectral results, we also conclude that the ligand field strength around the eight-coordinate Mn^{2+} in the sandwich $[Mn(12C4)_2]^{2+}$ species is closer to that of Mn^{2+} in T_d environments.

Figures 3c−e shows that the 410 nm peak is a poorly resolved doublet; we attribute this absorption to the transition $^4E(^4G) \leftarrow {}^6A_1$ of $[Mn(12C4)_2]^{2+}$. Normally the Mn^{2+} ($^4A_1$,^4E) ← $^6A_1$ transitions are narrow and nearly resonant; in $[Mn(12C4)_2]^{2+}$ these transitions have noticeably different energies ($^4E(^4G) \leftarrow {}^6A_1$ (410 nm) and $^4A_1(^4G) \leftarrow {}^6A_1$ (432 nm)) even under the low spectral resolution conditions of our experiment (maximum resolution, ±2 nm). Two weak peaks, one at 255 and the other at 260 nm, in the excitation spectra (λ_{em} = 585 or 546 nm) of **7**−**9** (Figure 3c−e), have greater intensity compared to the excitation spectra of **3** (Figure 3a,b). We speculate that these peaks may have been generated by the splitting of the $^4T_2(^4F)$ state of the $[Mn(12C4)_2]^{2+}$ cation.

Luminescence Decay Dynamics of Compounds 3, 7, and 8. Encouraged by the above luminescence spectral results, we studied the energy transport dynamics of crystals of **3**, **7**, and **8** in order to gain more insight into the $[Mn(12C4)_2]^{2+}\cdots MnBr_4^{2-}$ electronic interactions. Pulsed laser excitation of **3**, **7**, and **8** at 360, 410, and 479 nm produced similar luminescence decay kinetics. All decay curves were subsequently recorded following excitation into the $^4T_1(^4G)$ state of $MnBr_4^{2-}$ at 479 nm.

The 77 K emission from the $MnBr_4^{2-}$ species in **7**, where the concentration of these anions is very low, monitored at about 520 nm decays nonexponentially and is largely quenched. For example, the tail decays at a faster rate of roughly 6×10^4 s^{-1} compared to the normal decay rate[20,37,38] of $MnBr_4^{2-}$ emission of roughly $k_s \approx 2.8 \times 10^3$ s^{-1}. Consistent with the low population of $[Mn(12C4)_2]^{2+}$ traps in **8** (compared to **7**) and the higher abundance of diamagnetic $[Mg(12C4)_2]^{2+}$ cations, complicated decay kinetics of the $MnBr_4^{2-}$ 77 K emission from **8** still prevail, but quenching is considerably diminished compared to the high levels found in **7** (vide supra). For instance, the tail of the $MnBr_4^{2-}$ 77 K emission from **8** decays at a normal rate of roughly 3×10^3 s^{-1}, compared to ca. 6×10^4 s^{-1} for **7**. By contrast, for compound **3** in which the concentrations of both $MnBr_4^{2-}$ energy donors and $[Mn(12C4)_2]^{2+}$ acceptors are high, luminescence of the $MnBr_4^{2-}$ species (λ_{em} = 520 nm) is largely quenched and follows nonexponential decay kinetics. Consequently, the tail of **3**

(34) Furlani, C.; Furlani, A. *Inorg. Nucl. Chem.* **1961**, *19*, 51.
(35) Cotton, F. A.; Goodgame, D. M. L.; Goodgame, M. *J. Am. Chem. Soc.* **1962**, *84*, 167.
(36) Foster J. J.; Gill, N. S. *J. Chem. Soc. A* **1968**, 2625.
(37) Wrighton, M.; Ginley, D. *Chem. Phys.* **1974**, *4*, 295.
(38) Vala, M. T.; Ballhausen, C. J.; Dingle, R.; Holt, S. L. *Mol. Phys.* **1972**, *23*, 217.

decays at a higher rate of ca. 8×10^4 s^{-1} compared to both the frequently encountered natural $MnBr_4^{2-}$ luminescence decay rate (k_s) of ca. 2.8×10^3 s^{-1} [20,37,38] and the corresponding value (ca. 3×10^3 s^{-1}) for **8**. The similarities in the 77 K decay rates of $MnBr_4^{2-}$ emission from **3** and **7** are due to the presence of large amounts of $[Mn(12C4)_2]^{2+}$ excitation traps in both compounds. At 300 K, $MnBr_4^{2-}$ emission from **3** is weak, fast, and obscured by the more intense and longer lived $[Mn(12C4)_2]^{2+}$ luminescence. A variable-temperature (10−300 K) study of the emission decay behavior of $MnBr_4^{2-}$ revealed weakly temperature dependent decay curves which are complicated for $10 < T < 77$ K but single exponential for $T > 100$ K. Decay rates varied from ca. 4.8×10^4 s^{-1} at 10 K to ca. 8×10^5 s^{-1} at 300 K. An Arrhenius plot utilizing rates derived from single-exponential curves is linear and gives a phonon-type, thermal barrier of only ca. 67 ± 7 cm^{-1} which is similar to the ν_2 (bending) vibrational absorption for MBr_4^{2-} ions.[20]

The long-lived emission of **7** decays very slowly at rates of 1.3×10^2 and 3.0×10 s^{-1} at 300 and 77 K, respectively. The long-lived emission of **8**, in which the concentration of $[Mn(12C4)_2]^{2+}$ is low, is too weak to measure with our setup at 300 K, but this emission monitored at 550 nm and 77 K decays exponentially at roughly 3×10 s^{-1} as found for **7**. The long-lived emission of **3** monitored at $\lambda_{em} = 550$ nm follows exponential decay kinetics with a rate of only 3×10 s^{-1} at 77 K, the decay behavior at 300 K being more complex but with an exponential tail corresponding to a decay rate of about 3.6×10^2 s^{-1}. Compared to the behavior of **7**, the long-lived emission of **3** at 300 K is significantly quenched, which indicates active back $Mn(12C4)_2]^{2+}$-to-$MnBr_4^{2-}$ energy transfer at room temperature. There was no rise on the decay curves of the long-lived emission of **3**, **7**, and **8** when monitored at wavelengths of $\lambda_{em} > 550$ nm, which suggests that $MnBr_4^{2-}$-to-$[Mn(12C4)_2]^{2+}$ energy transfer is fast. Since the strengths of the crystal fields around the Mn^{2+} ions in $MnBr_4^{2-}$ and $[Mn(12C4)_2]^{2+}$ appear to be similar, the spectral overlap between the absorption of $[Mn(12C4)_2]^{2+}$ and the emission of $MnBr_4^{2-}$ is expected to be poor. Since the temperature dependence of the quenching process of $MnBr_4^{2-}$ emission was insignificant, we turned to the temperature evolution of the decay behavior of the long-lived emission of **3** for more insight on the $MnBr_4^{2-}$-$[Mn(12C4)_2]^{2+}$ electronic interactions.

The decay curves of the long-lived emission from **3** ($\lambda_{exc} = 479$ nm; $\lambda_{em} = 550$ nm) are perfectly exponential up to 220 K but very complex for $240 \leq T < 280$ K. Simpler decay behavior approximating to double exponential kinetics is seen at 330 and 320 K; the short-lived component decays at roughly $(3-5) \times 10^3$ s^{-1} while the long-lived one decays at roughly 4×10^2 s^{-1}. For $T < 120$ K, the decay rates differ marginally (28−33 s^{-1} at 56−120 K, respectively); the corresponding thermal barrier is small (180 ± 40 cm^{-1}). Greater temperature dependence is found for $T > 120$ K; the thermal barrier to quenching of the long-lived emission derived from exponential decay curves ($120 < T < 220$ K) or tails ($T > 220$ K) is 700 ± 30 cm^{-1}. Whereas the thermal barrier of 180 ± 40 cm^{-1} is close to the ν_1 (symmetric) stretch of $MnBr_4^{2-}$ and there are suitable vibrations of 12C4 and $(CH_3)_4N^+$ which can be attributed to the thermal barrier of 700 cm^{-1}, more information seems essential for a full understanding of the complex luminescence decay behavior of **3**.

We conclude that emission from the sandwich species $[Mn(12C4)_2]^{2+}$ is strongly sensitized via fast $MnBr_4^{2-}$-to-$[Mn(12C4)_2]^{2+}$ energy transfer for $T = 10$ K but back $[Mn(12C4)_2]^{2+}$-to-$MnBr_4^{2-}$ energy transfer is also active, especially for $T > 120$ K. Since the partially quenched emission of $[Mn(12C4)_2]^{2+}$ follows exponential decay behavior ($T < 220$ K), energy migration on the $[Mn(12C4)_2]^{2+}$ sublattice should also be fast so that the combined $[Mn(12C4)_2]^{2+}$-to-$[Mn(12C4)_2]^{2+}$ and $[Mn(12C4)_2]^{2+}$-to-$MnBr_4^{2-}$ energy transport behavior is in the dynamic regime.[26]

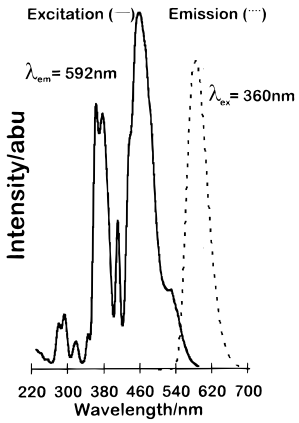

Figure 4. The 77 K uncorrected emission and excitation spectra of the deuterated derivative of **5**.

Luminescence of Compounds 4, 5, and 6. The $[Mn(15C5)(H_2O)_2]^{2+}$ complex ion in $[Mn(15C5)(H_2O)_2][TlBr_5]$ **(4)** emits weakly, while stronger emission is obtained for the deuterate $[Mn(15C5)(D_2O)_2]^{2+}$ in $[Mn(15C5)(H_2O)_{2-x}(D_2O)_x][TlBr_5]\cdot((H_2O)_{2-x}(D_2O)_x)$ ($0 < x < 2$) (**6**). However, $[Mn(15C5)(D_2O)_2]^{2+}$ in the deuterated derivative of $[Mn(15C5)(H_2O)_2][MnBr_4]\cdot 2H_2O$ (**5**) gives an intense orange emission when excited in the UV. The emission at 77 K peaks (Figure 4) at 592 nm and decays exponentially at a rate of ca. 1.8×10^3 s^{-1} for deuterated derivatives of both **4** (i.e., **6**) and **5** (i.e., **5** recrystallized from D_2O). The excitation spectrum of the deuterated derivative of **5** ($\lambda_{em} = 592$ nm) is dominated by $MnBr_4^{2-}$ absorptions (Figure 4), but absorptions at 317, 342, 406, and 531 nm not typical of $MnBr_4^{2-}$ are also evident. We assign these absorptions (using $\Delta \approx 4500$ cm^{-1}) to direct $^2T_2(^2I) \leftarrow {}^6A_1$, $^4T_1(^4P) \leftarrow {}^6A_1$, $^4E(^4G) \leftarrow {}^6A_1$, and $^4T_1(^4G) \leftarrow {}^6A_1$ transitions, respectively, of the seven-coordinate $[Mn(15C5)(D_2O)_2]^{2+}$ species.[38] The $^4E(^4G)$ and $^4A_1(^4G)$ states have noticeably different energies, 410 and 436 nm in the deuterated derivative of **5**. The relatively broad $^6A_1$-to-$^2T_2(^2I)$ transition is doubly spin forbidden and is rarely seen[38] with such high intensity as exhibited by the $[Mn(15C5)(D_2O)_2]^{2+}$ ion. Covalence and spin−orbit coupling considerations do not satisfactorily explain the observed high intensities here.

We thus conclude that the good spectral overlap between the $^4T_1(^4G) \rightarrow {}^6A_1$ emission of energy-donating $MnBr_4^{2-}$ ions (usually at ca. 510−535 nm) with the $^4T_1(^4G) \leftarrow {}^6A_1$ absorption (531 nm) of the energy-accepting seven-coordinate $[Mn(15C5)(H_2O)_2]^{2+}$ species in **5** provides an efficient mechanism for $MnBr_4^{2-}$ -to-$[Mn(15C5)(H_2O)_2]^{2+}$ energy transfer. More luminescent seven-coordinate manganese(II) compounds are being sought in an attempt to shed more light on the electronic properties of such systems.

Conclusion

The emission features of **3**−**9** do show conclusively that Mn^{2+} emission ($^4T_1(^4G) \rightarrow {}^6A_1$) is not restricted to T_d and O_h coordination environments only; Mn^{2+} ions in seven- and eight-fold coordination environments do emit too. Therefore manganese(II) sites which have effective crystal fields of lower than

T_d symmetry can be expected to contribute to emission from **1**; it is reasonable to invoke them to explain the unusual emission behavior of **1**, **2,** and related complexes.[20] To our knowledge, compounds **3**−**9** provide the first examples of manganese(II) $^4T_1(^4G) \rightarrow {}^6A_1$ emission in stoichiometric compounds in which the Mn^{2+} cation is in noncubic coordination environments.

Acknowledgment. We thank the Chemistry Department of the University of the West Indies (UWI) for a demonstratorship for H.O.R., the UWI R & P and Post-graduate grants committees for funds to purchase a laser system, and the UWI-British Council CICHE program for supporting the University of the West Indies−Imperial College Collaboration. We are also grateful for assistance from the InterAmerican Development Bank-UWI Development program which was used to purchase the helium refrigerator.

Supporting Information Available: Tables of crystal data, atomic coordinates, all bond distances and angles, anisotropic displacement parameters, and hydrogen coordinates for **3** (6 pages). Ordering information is given on any current masthead page.

IC980035O